

## LOW DRIVING VOLTAGE FOR FLEXIBLE ORGANIC LIGHT EMITTING DIODES BASED ON TRANSPARENT ANODE

M. V. MADHAVA RAO<sup>a,b,c\*</sup>, Y. K. SU<sup>a</sup>, Y.C. LIU<sup>a</sup>, T.S. HUANG<sup>a</sup>

<sup>a</sup>*Institute of Microelectronics, Department of Electrical Engineering, and Advanced Optoelectronic Technology Center, National Cheng Kung University, Tainan 701, Taiwan.*

<sup>b</sup>*Department of Physics, University College of Science, Osmania University, INDIA*

<sup>c</sup>*Department of Materials Engineering, Soonchunhyang University, Republic of Korea*

We reported a flexible organic light emitting diodes (OLED) with a structure of PET/PHEMA /Ag (20 nm)/MoO<sub>2</sub> (5 nm)/NPB (40 nm)/Alq<sub>3</sub>:1% C545T (40 nm)/Alq<sub>3</sub> (30 nm)/LiF/Al. To improve the performance of the Flexible OLED, a semitransparent anode (Ag) and insulating polymer buffer layer (PHEMA) into the polymer substrate. Our flexible OLED devices show that low operating voltages, low turn-on voltage (defined for voltage to obtained a luminance of 1 cd/m<sup>2</sup>) of 2.54 V, 14.6 cd/m<sup>2</sup> at 3.54 V, 100 cd/m<sup>2</sup> at 4.68 V and 150 cd/m<sup>2</sup> at 5V, respectively. The flexible anode effectively enhanced the probability of hole-electron recombination due to an efficiency hole injection into and charge balance in an emitting layer. By comparing with a reference OLED using ITO on PET, it is verified that our flexible OLED shows a better electroluminescence performance. An OLED on a flexible substrate is fabricated to demonstrate the potential use of a semitransparent Ag electrode as a transparent conducting electrode.

(Received June 13, 2016; Accepted August 11, 2016)

*Keywords:* OLED; electroluminescent; flexible electrode; surface morphology

### 1. Introduction

Organic light-emitting devices (OLEDs) based on small molecules and conjugated polymers have gained great interest due to their potential to provide low-cost and high-efficiency solutions for applications such as solid-state lighting and large area displays. Significant development efforts have focused on electronic display circuitry and light-emitting devices on flexible substrates driven by increasing consumer demand for inexpensive, light-weight and portable devices [1-4]. Flexible OLEDs fabricated on flexible substrates provide ability to conform, bend or roll a display into any shape, and also will give possibility of fabricating displays by continuous roll processing. Flexible OLEDs were made on plastic substrates by many research groups. Flexible electronic systems and applications such as electronic newspapers, wearable electronics and displays, require flexible electrodes with low cost production [5-7]. Indium-tin oxide (ITO) has been so far the most common transparent electrode material because of its high work function, high transparency and availability. However, ITO is not an ideal choice for fully flexible electronic devices because devices fabricated on flexible plastic substrates with ITO break too easily as a result of failure of the ITO as they are bent [8-10]. Therefore, a great deal of interest has been devoted to the replacement of ITO for fully flexible devices. Polymeric anodes, metal anodes, modified oxide anodes, carbon nanotube sheet anodes and nanocomposite anodes have been explored as alternatives to transparent ITO anodes.

Polymers such as polyethylene terephthalate (PET) and polyethylene naphthalate (PEN) are promising materials for use as flexible substrates, having many advantageous properties

---

\*Corresponding author: madhavmora@yahoo.com

including transparency, light weight, flexibility, chemical resistance and low coefficients of thermal expansion [10]. Generally, plastic substrates have good properties such as high transmittance and flexibility, however, they suffered from low glass transition temperature ( $T_g$ ) below 200 °C and decreased the lifetime of FOLEDs because of crystallization of organic materials at around 200 °C by diffused moisture and/or oxygen through the plastic substrate [11,12]. For the purpose of reducing moisture permeability through the plastic substrate, it was attempted to insert a barrier layer between the FOLEDs and the plastic substrates. Burrows et al. utilized the layers of poly-acrylate between multiple layers of the inorganic materials such as  $\text{SiO}_2$ ,  $\text{Si}_3\text{N}_4$ , and  $\text{Al}_2\text{O}_3$  [13]. However, there is a limit to various deposition processes and flexibilities. The low flexibility of inorganic films can diffuse moisture and/or oxygen in atmosphere through the micro cracks or pinholes [10,14].

Polymer light-emitting diodes based on shape memory polymer (SMP) substrates by using a single-walled carbon nanotube/polymer composite electrode as an ITO replacement, first reported by Yu and et al [15,16]. These devices produced a maximum current efficiency of 1.24 cd/A at 200 cd/m<sup>2</sup> with a turn-on voltage of 4.8 V, and a maximum luminance of 300 cd/m<sup>2</sup>. Gaj and et al [17], reported that inverted top-emitting OLEDs fabricated in biocompatible SMP substrates produced current efficacies of 3.3 cd/A at a high luminance of 1000 cd/m<sup>2</sup> with a low turn-on voltage of 3.4 V. Moreover, these devices can produce a maximum luminance of over 30,000 cd/m<sup>2</sup>. These results demonstrate an alternative method to fabricate flexible electronics using conformable substrates and can be extended to a wide range of potential applications ranging from bio-engineering to flexible displays and lighting.

A simple ITO film for transparent conductors has been using as of ITO–metal–ITO multilayers, has gained much attention as promising flexible anode materials for flexible OLEDs because the dielectric/metal/dielectric(DMD) multilayer system can suppress the reflection from the metal layer and obtain a selective transparent effect [18-20]. This structure is composed of a thin Ag layer sandwiched between two ITO layers. It was suggested that efficient plasmon coupling between Ag and ITO could enhance visible transparency greater than 90% [21,22]. Using this dielectric/metal/dielectric stack system, Fahland and et al. demonstrated that an ITO–Ag–ITO multilayer on a PET substrate and maximum transmittance of 80% at optimized conditions [23]. Lewis et al. also reported that electrical and mechanical properties of the ITO–Ag–ITO anode could be remarkably improved by the effect of a continuous Ag layer between the ITO anode [24]. They showed that the performance of flexible OLEDs fabricated on an ITO–Ag–ITO anode is better than that of flexible OLEDs fabricated on an ITO/glass sample. Although optical and electrical properties of ITO–Ag–ITO multilayers have been reported, characteristics of indium zinc oxide (IZO)–Ag–IZO (IAI) stacks and the performance of IAI-based flexible OLEDs have been reported [20]. IZO films have recently been recognized as promising anode materials for flexible OLEDs due to their conductivity, high transparency, excellent surface smoothness, low process temperature, and mechanical stability [24]. However, DMD- transparent electrodes based on ZnS/Ag/ZnS and  $\text{WO}_3/\text{Ag}/\text{WO}_3$  electrodes turned out inefficient mainly due to poor carrier injection properties of Ag/Zn or Ag/ $\text{WO}_3$  systems. Moreover, all those devices were fabricated on conventional glass substrates, and thus the potential of DMD electrodes for flexible OLEDs was not known [25,26].

In this study, a semi-transparent Ag electrode on the PET substrate was demonstrated. The fabricated semitransparent Ag electrode showed high transmittance in the visible range and good electrical conductivity. As an application, a flexible OLED was fabricated using a semitransparent Ag electrode as the anode to replace the conventional ITO/PET electrode.

Impressive luminance, current density, and efficiency were achieved incorporating Poly(2-hydroxyethyl methacrylate)( PHEMA)[27,28] layer in between the substrate and Ag anode. The current density, luminance, current efficiency and electroluminescence spectra (EL) of flexible OLED were characterized by comparison to conventional OLED with ITO anode on PET substrate

## 2. Experimental

Poly(ethylene terephthalate) (PET) films with a thickness of 175  $\mu\text{m}$  were adopted as the flexible substrate. The 120  $\text{ohm/sq}$  sheet resistance of the PET coated with ITO films was used as reference. The materials, PHEMA (99.9%), Ag,  $\text{MoO}_3$  (99.5%), NPB, tris(8-hydroxyquinolinato)aluminium ( $\text{Alq}_3$ ), lithium fluoride (LiF), Al and fluorescent green dye of 10-(2-benzothiazolyl)-1,1,7,7-tetramethyl-2,3,6,7-tetrahydro-1H,5H,11H-benzo[1]pyrano-[6,7,8-ij]quinolizin-11-one (C545T), were purchased from Sigma-Aldrich. We used the device structure of PET/ITO/ $\text{MoO}_3$  (5 nm)/NPB (40nm)/ $\text{Alq}_3$ :1% C545T (40 nm)/ $\text{Alq}_3$  (30 nm)/LiF (0.5nm)/Al [ITO], PET/Ag (20nm)/ $\text{MoO}_3$  (5 nm)/NPB (40nm)/ $\text{Alq}_3$ :1% C545T (40 nm)/ $\text{Alq}_3$  (30 nm)/LiF (0.5nm)/Al [Ag], PET/PHEMA (1000K molecular weight)/Ag (20 nm)/ $\text{MoO}_2$  (5 nm)/NPB (40nm)/ $\text{Alq}_3$ :1% C545T (40 nm)/ $\text{Alq}_3$  (30 nm)/LiF (0.5nm)/Al (200 nm) [Ag/PHEMA(1000K)] and PET/PHEMA (20K molecular weight)/Ag (20 nm)/ $\text{MoO}_2$  (5 nm)/NPB (40 nm)/ $\text{Alq}_3$ :1% C545T (40 nm)/ $\text{Alq}_3$  (30 nm)/LiF (0.5nm)/Al (200 nm) [Ag/PHEMA(20K)]. Prior to device deposition, the flexible PET substrates were cleaned with acetone and ethanol by using ultrasonic bath, rinsed with deionized water, and then dried in an oven at 80°C for 10 min. Then the pre-prepared flexible PET substrates were transferred into a glove box to spin coat a PHEMA buffer layer or a vacuum chamber to thermally evaporate different thicknesses of the  $\text{MoO}_3$  buffer layer. After that a 20-nm thick Ag film was deposited onto the buffer layer or the pure PET substrate as the bottom anode, followed by a 5 nm  $\text{MoO}_3$  hole injection layer. The organic layers were then sequentially deposited. All organic layers and electrodes were grown by thermal evaporation in a high vacuum system under a pressure of less than  $5 \times 10^{-4}$  Pa. The deposition rates of the organic layers and the electrodes were about 0.1–0.2 nm/s and 0.2–0.4 nm/s, respectively. The deposition of both hosts and guests was controlled with independent quartz crystal oscillators. After cooling for about one hour, the devices were transferred into a glove box to measure the EL characteristics. The active area of our device was  $6\text{mm}^2$  and the devices were encapsulated in a glove box. Figure 1 shows the schematic diagram of the Flexible OLED. The luminance–voltage–current density (L–V–J) characteristics of the OLED devices were measured by a dc current/voltage source meter (Keithley 2400), while the brightness was monitored with a spectrophotometer (Photo Research PR655). Atomic Force Microscopy (AFM, DI dimension 3100) was used to monitor the surface morphology of films. The surface topography images of the films Ag, Ag/PHEMA(100K) and Ag/PHEMA(20K) coated PET substrate films. The AFM images are measured with  $3 \times 3 \mu\text{m}^2$  area.

AFM is the surface described by cantilever during scan, due to the tip-sample interaction. This leads to the equiforce surface image limited by a convolutive interaction. Because the roughness values are influenced by tip, scan size. The main parameters for profile evaluation are defined as [29]:

Average Roughness ( $R_a$ ) — the arithmetic average of a deviation  $y$ , from the center line is:

$$R_a = \frac{1}{L} \int_0^L |y| dx$$

Root-Mean-Square Roughness ( $R_{rms}$ ) is the root-mean-square deviation from center line:

$$R_{rms} = \left( \frac{1}{L} \int_0^L y^2 dx \right)^{1/2}$$

For each sample, the rms roughness and average roughness as defined in [29] were evaluated.

Al(200nm)	Al(200nm)	Al (200nm)
LiF(0.5nm)	LiF(0.5nm)	LiF (0.5nm)
Alq <sub>3</sub> (30nm)	Alq <sub>3</sub> (30nm)	Alq <sub>3</sub> (30nm)
Alq <sub>3</sub> :C545T	Alq <sub>3</sub> :C545T	Alq <sub>3</sub> :C545T
NPB(40nm)	NPB(40nm)	NPB(40nm)
MoO <sub>3</sub> (5nm)	MoO <sub>3</sub> (5nm)	MoO <sub>3</sub> (5nm)
ITO		PHEMA
PET	PET	PET

Fig. 1. Device configuration of flexible OLED structure.

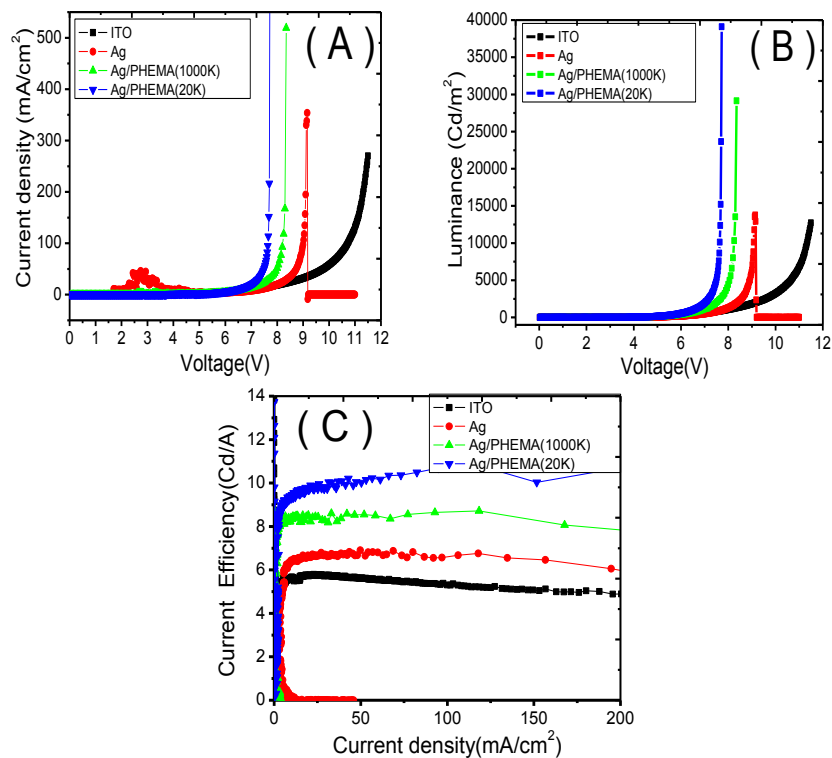


Fig.2 ( A ) Current density-Voltage ( B ) Luminance-Voltage, ( C ) Current efficiency-Current density characteristics of the flexible OLED devices

### 3. Results and discussions

Fig.2(A) shows the current-voltage characteristics of the flexible OLED fabricated on Ag/PHEMA(20K), Ag/PHEMA(100K), Ag and ITO devices respectively. The current density of a flexible OLED fabricated on the Ag/PHEMA(20K) anode is much higher than that of a flexible OLED fabricated on an ITO/PET anode device at the same voltage after a turn-on of flexible OLEDs. The higher current density of flexible devices on the Ag/PHEMA(20K), Ag/PHEMA(100K), Ag anode with applied voltage is explained a high leakage current at a forward bias before the turn-on due to a large shunt resistance, indicating leaky interface between the ITO and the organic layer. Fig. 2(B) indicates that the luminance-voltage curves of the flexible OLEDs on the Ag/PHEMA(20K), Ag/PHEMA(100K), Ag anode devices also exhibits much higher luminance than that of a flexible OLED on the ITO anode device. The luminance of 39103 cd/m<sup>2</sup> achieved by the present Ag/PHEMA(20K) device easily meets the requirements for many displays applications, where light intensities of 100-300 cd/m<sup>2</sup> are required. Although the present

device luminance does match those found devices using ITO/glass anodes in similar structures, the low turn-on voltage and brightness achieved are encouraging. For instance, the current density at 7V was 9.8, 7.8, 13.5 and 20 mA/cm<sup>2</sup> for flexible OLEDs on ITO, Ag, Ag/PHEMA(100K), and Ag/PHEMA(20K) devices respectively. The success in forming a semitransparent Ag layer, the use of Ag only anode in an OLED usually results in a poor device performance due to the existence of a large barrier for the hole injection. Li et al[30], demonstrated that the hole injection can be significantly enhanced by inserting a CFX film between Ag and organic film, which provides the feasibility to form an ITO-free OLED using bilayer anode of Ag/CFX. The current efficiency versus voltage characteristics of flexible devices are shown in Fig.2 ( C ). Interesting phenomenon we observed is that the relatively stable efficiency values were maintained over the current density ranges of 10-200 mA/cm<sup>2</sup> for the Flexible OLED devices. The maximum efficiency values of Ag/PHEMA(20K) (10.96 cd/A, 113 mA/cm<sup>2</sup>), Ag/PHEMA(100K) (8.7 cd/A, 118 mA/cm<sup>2</sup>), Ag(6.9 cd/A, 50mA/cm<sup>2</sup>) and ITO(5.73 cd/A, 36 mA/cm<sup>2</sup>) obtained to Flexible OLED devices. This can be attributed to a better balance of holes and electrons in the recombination zone when the current density was increase. We have prepared simple method for the fabrication of high performance flexible OLED devices using Ag thick layer as the anode after the surface modification of polymer substrate. Impressive device luminescence, current density, and luminance efficiency were achieved incorporating PHEMA buffer layer in between PET substrate and Ag layer.

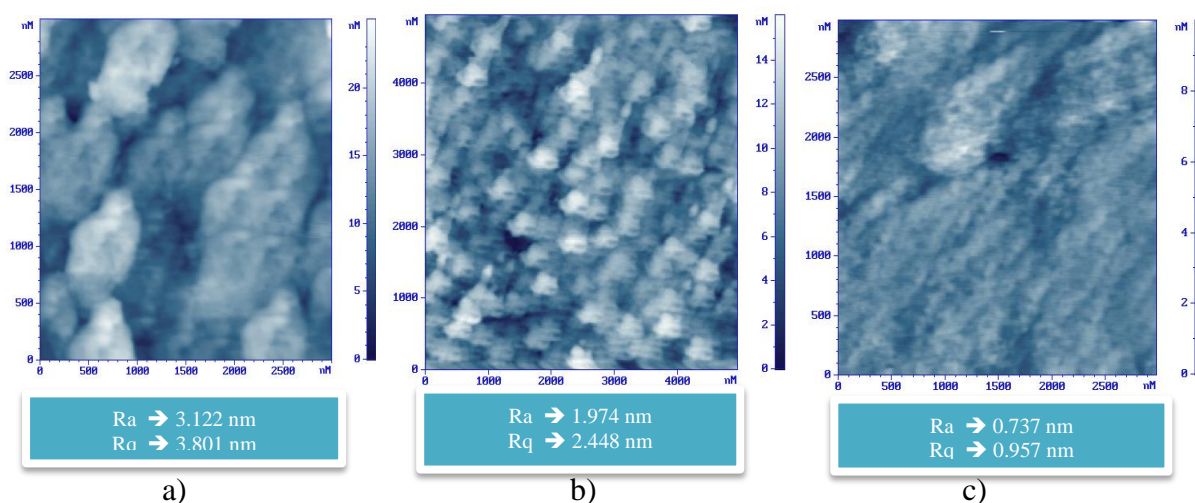


Fig.3. AFM images of ( A ) Ag ; ( b ) Ag/PHEMA(100K); ( c ) Ag/PHEMA(20K) coated on PET substrate

Fig. (3) shows the topographical images that present the surface root mean square (RMS) roughness for only Ag, Ag/PHEMA(100K) and Ag/PHEMA(20K) coated PET substrate films, As shown in AFM images of sample. The average RMS of the surface roughness is only Ag of 3.122 nm , PHEMA(100K) of 1.974 nm and PHEMA(20K) of 0.737 nm respectively. The as-deposited Ag has a surface RMS roughness of 3.122 nm. After spin coating PHEMA(100K), PHEMA(20K), the surface exhibits a reduced roughness of 1.974 and 0.737 nm. The surface roughness is significantly decreased from 3.122 to 0.737 nm due to uniformity of PHEMA buffer layer. This reveals that Ag has a relatively poor smooth surface. In the Ag only surface, the surface morphology is island structure. In addition, there are Ag/PHEMA(100K) and Ag/PHEMA(20K) for the low RMS roughness of surface, the structure of island have fallen away little. In fact, the smooth uniformity of film surface for improving interface contact of the Ag/PHEMA(20K) layer with organic layer is important for the injection and transmission properties of carrier. Therefore, carrier can be easily injected from Ag/PHEMA(20K) to organic mediums when the device is properly biased[31-33].

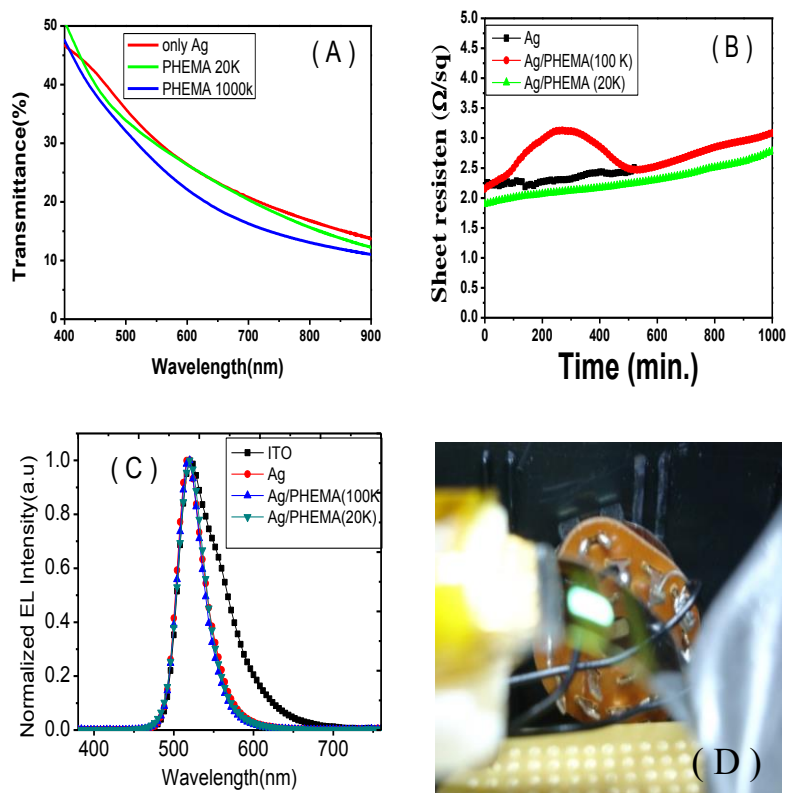


Fig.4 (A) Transmittance – Wavelength (B) Sheet resistance-time (C) Normalized EL emission spectra of the flexible devices (D) A photo image showing a flexible OLED device fabricated in our experiment

Fig. 4(A) shows optical transmission spectra of a Ag/PET, PHEMA(100K) and PHEMA(20K) substrates. The maximum transmittance at 545 nm was 31% (Ag/PET), 30.2% (PHEMA(100K) and 27.2% (PHEMA(20K) substrates and average transmittance in the visible range(450-650 nm) was around 32% (Ag), 31% (PHEMA(100K) and 28% (PHEMA(20K). Due to negligible optical losses in the hole transport layer, the hole injection layer thickness can be increased further without affecting transmittance of the OLEDs. The thick layer device Ag(20 nm) shows 1-4% higher transmittances than the device PHEMA(20K) and PHEMA(100K), One should note that the superior features of Ag films were obtained by simple thermal evaporation.

Fig.4 (B) shows that sheet resistance versus time for different anode films under 10 mV constant voltage. There are no extreme changes for long time test. This results shows that use of PHEMA to modify the silver film can reduce the sheet resistance to about 2 ohm/sq. This is main reason to decrease the turn-on voltage. The high performance of flexible OLEDs on the Ag/PHEMA(20K), Ag/PHEMA(100K), Ag anode devices can be attributed to the low sheet resistance and high transmittance caused by the insertion of Ag metal layer along with PHEMA buffer layer. This improvement indicates the validity of the anode preparation developed in this work.

The electroluminescence (EL) spectra of the flexible OLED with Ag/PHEMA(20K), Ag/PHEMA(100K), Ag anode and normal ITO anode at the same applied voltage were shown in Fig.4( C ). The devices with Ag/PHEMA(20K), Ag/PHEMA(100K), Ag device anode showed a typical EL spectrum of the Alq<sub>3</sub> based OLED fabricated on the ITO anode with the emission peak wavelength of 520 nm. On the other hand, the device with the ITO anode showed an EL spectrum with increased intensities above 520 nm. The ITO free flexible anode which has relatively very low transmittance at the long wavelength region seems to have partially cut off the light emitting from the devices. Also, this cut-off contributed to decrease the emission efficiency of the device. When an optimized Ag/PHEMA(20K), Ag/PHEMA(100K), Ag anode which has electrically superior characteristics than the ITO anode was employed the Flexible OLED devices exhibited a

largely enhanced performance in terms of brightness and current efficiency without altering in the EL spectrum[4,10].

Fig.4 ( D) shows that a photo image of a flexible OLED on PET substrate. The device still performance after several repeated bending, suggesting that there is no significant stress-induced change in the characteristics of the OLEDs fabricated on PET substrate. The results demonstrate the feasibility of fabricating flexible displays using a variety of plastic substrates in the flexible device structures enable a display to conform, bend, or roll into any shape and thus make possible other product concepts.

We can see that the Ag/PHEMA(20K) device with PHEMA buffer layer has a threshold voltage (2.54 V) lower than that of the Ag devices (3.52 V) and about eight times higher than the brightness under the same voltage. At 7.72 V, the emission of the device with the Ag/PHEMA(20K) film reaches 39103 cd/m<sup>2</sup> while the device without the PHEMA film Ag only has a brightness of 970 cd/m<sup>2</sup>. The Ag/PHEMA(20K) coated substrate also enhances the device efficiency from 6.7 cd/A to 10.91 cd/A. This is a impressive improvement. Many studies based on glass substrates show that different ITO surface morphologies greatly affect the performances of OLEDs. These results prove that the organic films will be continuous, compact and have less rms roughness when fabricated on the conductive substrate with PHEMA buffer layer. Firstly, high quality thin film for an organic hole transport layer can effectively enhance the carrier injection and transmission. Secondly, the insertion of PHEMA buffer layer eliminates grain boundaries existing densely on the PET substrate, and enlarges the top plane area which is able to make a good contact with the organic layer. Therefore, the reduction roughness of ITO substrate increases the current density flowing through the OLEDs. Thirdly, the improvement of optical transmittance of the complex substrate can also increase the efficiency of flexible OLEDs[4,10].

#### 4. Conclusions

In summary, we successfully fabricated a flexible OLED device consisting of PET/PHEMA (20K)/Ag (20 nm)/MoO<sub>2</sub> (5 nm)/NPB (40 nm)/Alq<sub>3</sub>:1% C545T (40 nm)/Alq<sub>3</sub> (30 nm)/LiF/Al. Ag/PHEMA(20K) anode enhanced a hole injection from anode to a hole transport layer in the flexible OLED and more effectively increased a probability of hole-electron recombination due to improving the balance of charge carriers between anode/hole transport layer and electron transport layer. The flexible OLED showed a maximum luminance and the current efficiency of the flexible OLED are 39103 cd/m<sup>2</sup> at 7.7 V and 10.91 cd/A at 7.6 V respectively, these data are better than those devices of using the ITO, Ag and PHEMA (100K) devices, luminance and current efficiencies enhancement factor are 9.2/2.1, 8.9/1.6, and 3.4/1.25. The corresponding flexible device revealed the remarkable performance, including the low driving voltages of 2.54 V ( 1 cd/m<sup>2</sup>), and 4.68 V for 100 cd/m<sup>2</sup>. The low driving voltage and enhanced luminance and current efficiencies pave the way for the practical applications of these devices in portable displays and lighting.

#### Acknowledgements

We would like to thanks the Research and Development, National Cheng Kung University for financial support.

#### References

- [1] Q. Wang, D. Ma, Chem. Soc. Rev. **39**, 2387 (2010)
- [2] M.V. Madhava Rao, T.S. Huang, Y.K.Su, M.L. Tu, C.Y. Huang, and S.S. Wu, Nano-Micro Letters, **2**,49 (2010)
- [3] M.V. Madhava Rao, Y.K. Su, T.S. Huang, and Y.C.Chen, Nano-Micro Letters, **2**, 242 (2010)

- [4] X. Xu, G. Yu, Y. Liu, D. Zhu, *Displays* **27**, 24 (2006)
- [5] G. Gu, P.E. Burrows, S. Venkatesh, S.R. Forrest, and M.E. Thompson, *Optics Letters*, **22**, 172 (1997).
- [6] H. Lim, W.J. Cho, C.S. Ha, S. Ando, Y.K. Kim, C.H. Park, K. Lee, *Advanced Materials* **14**, 1275 (2002).
- [7] S.H. Kwon, S.Y. Paik, and J.S. Yoo, *Synthetic Metals* **130**, 55 (2002).
- [8] Y. He, J. Kanicki, *Appl. Phys. Lett.* **76**, 661 (2000).
- [9] Y. Hong, Z. He, N. S. Lennhoff, D. A. Banach, and J. Kanicki, *Journal Electron. Mater.*, **33**, 312 (2004).
- [10] M. H. Park, T.H. Han, Y. H. Kim, S. H. Jeong, Y. Lee, H. K. Seo, H. Cho, and T.W, Lee, *Journal of photonics for Energy* **5**, 053599 (2015)
- [11] L. Do, K. Kim, T. Zyung, H. Shim, J. Kim, *Appl. Phys. Lett.* **70**, 3470 (1997)
- [12] S.F. Lim, L. Ke, W. Wang, S.J. Chua, *Appl. Phys. Lett.* **78**, 2116 (2001)
- [13] P.E. Burrows, G.L. Graff, M.E. Gross, P.M. Martin, M.K. Shi, M. Hall, E.Mast, C. Bonham, W. Bennett, M.B. Sullivan, *Displays* **22**, 65 (2001)
- [14] R.S. Kumar, M. Auch, E. Ou, G. Ewald, C.S. Jin, *Thin Solid Films* **417**, 120 (2002)
- [15] Z. Yu, Q. X. Niu, Z. Liu, Q. Pei, *Adv. Mater.* **23**, 3989 (2011)
- [16] Z. Yu, Q. Zhang, L. Li, Q. Chen, X. Niu, J. Liu, and Q. Pei, *Adv. Mater.* **23**, 664(2011)
- [17] M.P. Gaj, A. Wei, C.F. Hernandez, Y. Zhang, R. Reit, W. Voit, S.R. Marder, B. Kippelen, *Organic Electronics* **25**, 151 (2015)
- [18] M. Bender, W. Seelig, C. Daube, H. Frankenberger, B. Ocker, J. Stollenwerk, *Thin Solid Films* **326**, 67 (1998)
- [19] J. Lewis, S. Grego, B. Chalamala, E. Vick, D. Temple, *Appl. Phys. Lett.*, **85**, 3450 (2004)
- [20] K.H. Choi, J.Y. Kim, Y.S. Lee, H.J. Kim, *Thin Solid Films* **341**, 152 (1999)
- [21] X. Liu, X. Cai, J. Mao, C. Jin, *Appl. Surf. Sci.* **183**, 103 (2001)
- [22] X. Liu, X. Cai, J. Qiao, J. Mao, N. Jiang, *Thin Solid Films* **441**, 200 (2003)
- [23] M. Fahl, P. Karlsson, C. Charton, *Thin Solid Films* **392**, 334 (2001)
- [24] J.-H. Bae, J.-M. Moon, J.-W. Kang, H.-D. Park, J.-J. Kim, W.J. Cho, H.-K. Kim, *J. of the Electrochem. Soc.* **154**, J81 (2007)
- [25] H. Pang, Y. Yuan, Y. Zhou, J. Lian, L. Cao, J. Zhang, X. Zhou, *J. of Luminescence* **122–123**, 587 (2007)
- [26] S.Y. Ryu, J.H. Noh, B.H. Hwang, C.S. Kim, S.J. Jo, J.T. Kim, H.S. Jeong, C.H. Lee, S.Y. Song, S.H. Choi, S.Y. Park, *Appl. Phys. Lett.* **92**, 022306 (2008)
- [27] H. Jintokua and H. Ihara, *Chem. Commun.* **50**, 10611 (2014)
- [28] X. Dai, Z. Zhang, Y. Jin, Y. Niu, H. Cao, X. Liang, L. Chen, J. Wang, and X. Peng, *Nature* **515**, 96 (2014)
- [29] C. Fluerau, S. Schrader, V. Zauls, H. Motschmann, B. Stiller, and R. Kiebooms, *Synth. Metals.* **111-112**, 603(2000)
- [30] Y. Q. Li, L. W. Tan, X. T. Hao, K. S. Ong, F. R. Zhu, and L. S. Hung, *Appl. Phys. Lett.* **86**, 153508 (2005)
- [31] M.V.Madhava Rao, Y.K. Su, T.S.Huang, and C.H.Yeh, *Nanoscale Research Lett.*, **4**:485 (2009)
- [32] M. V. Madhava Rao, Y.K.Su, T.S.Huang, M.L.Tu, S.S.Wu, C.Y.Huang, *J of The Electrochemical Society*, **157**, **8**, H832 (2010)
- [33] M.V. Madhava Rao, Y.K.Su, T.S. Huang, *ECS Solid State Letters*, **2(1)**, R5-R7 (2013)